

High-frequency acoustics and bio-optics in ecosystems research

D. V. Holliday, P. L. Donaghay, C. F. Greenlaw, J. M. Napp, and J. M. Sullivan

Holliday, D. V., Donaghay, P. L., Greenlaw, C. F., Napp, J. M., and Sullivan, J. M. 2009. High-frequency acoustics and bio-optics in ecosystems research. – ICES Journal of Marine Science, 66: 974–980.

The propagation of light and sound in the ocean's interior is modified by the presence of phytoplankton, zooplankton, fish, gas bubbles, and dissolved and suspended material. Information is encoded in the levels and spectral characteristics of acoustic and optical scattering and absorption. Using acoustics and optics allows us to study the distribution of marine life and learn about ecosystem-relevant processes. Two studies are highlighted. In the first, multifrequency, upward-looking echosounders deployed near autonomous, bio-optical profilers were used to track vertical migration and the formation and size structure of <1 m thick, zooplankton layers in relation to the biomass and size structure of thin phytoplankton layers. In the second, a multifrequency sonar was used to track the temporal (seasonal) evolution of zooplankton biomass and size structure in the Bering Sea at intervals of 20 min. This paper focuses on how advanced technologies are being used to observe processes, distributions, and behaviour of marine life that have, until now, been hidden, as it were, from biological oceanographers.

Keywords: acoustic oceanography, ecosystem monitoring, ocean optics, plankton, thin layers, zooplankton acoustics.

Received 5 August 2008; accepted 31 January 2009; advance access publication 8 May 2009.

D. V. Holliday: School for Marine Science and Technology, University of Massachusetts, Dartmouth, 5034 Roscrea Avenue, San Diego, USA. C. F. Greenlaw: 302 Tailwind Drive, Seguin, TX 78155, USA. P. L. Donaghay and J. M. Sullivan: Graduate School of Oceanography, University of Rhode Island, South Ferry Road, Narragansett, RI 02882, USA. J. M. Napp: National Oceanographic and Atmospheric Administration, National Marine Fisheries Service, Alaska Fisheries Science Center, 7600 Sand Point Way NE, Seattle, WA 98115, USA. Correspondence to D. V. Holliday: tel: +1 858 2795369; e-mail: vholliday@umassd.edu.

Introduction

An ecosystem is a community of living organisms and their physical environment, including the biological–biological and biological–physical–chemical interactions and processes that collectively allow the organisms and their habitat to function as a system. Ocean scientists and fishery managers have long advocated an “ecosystem approach” to the management of living marine resources, yet the practical and operational implications of implementing “ecosystem-based” management have proved far from simple. Even after several decades of discussion, what is implied by “an ecosystem approach to fishery management” varies considerably (ICES, 2004). Some have set forth general goals intended to maintain “healthy oceans” and preserve essential ecosystem services. Others describe more limited objectives, e.g. mandating harvesting methods that cause minimal harm to the marine habitat. Many view the “ecosystem approach” as the means to ensure that fish are harvested in a way that maintains sustainable yields and protects the overall ecosystem structure and function in the face of a changing environment that, realistically, includes both natural and human-induced variations. Protecting ecosystem structure and function involves directing attention not just to the living marine resources being harvested, but also to trophic levels that support and are supported by the harvested populations.

One of the most challenging tasks for ecosystem-based management is to gain an understanding of the critical processes that link the physical, chemical, and biological components of a marine ecosystem. Unlike terrestrial ecology, oceanographic observations of plants and animals and their physical and chemical

environment are rare at the time-scales fast enough, or long enough, to resolve the details needed to support accurate process modelling. If high-quality, comprehensive observations were available, they could result in a better scientific understanding of spatial distribution and how it changes, as well as a description of key processes regarding linkages and interactions in marine ecosystems. This, in turn, should lead to improved modelling at relevant trophic levels, including intra- and interspecies interactions, model testing and validation, and eventually, to an ability to predict the effects of changes in critical features of the physical environment and biological realms that constitute an ecosystem. Indeed, with better observations, many of the time-proved analysis tools of terrestrial ecology could become useful for marine-ecosystem management. In the marine environment, indirect observation is usually the norm, often employing technology-based tools, underwater acoustics, and underwater optics, for remote sensing.

The use of high-resolution sensors to examine fine-scale distributions, size structure, biophysical interactions, and *in situ* behaviour of phytoplankton, zooplankton, and micronekton is described here. These tools are capable of presenting fishery managers with data that quantify important ecosystem attributes and processes. Such information could eventually represent the first real-time boundary conditions for data-driven models with direct application to fishery management, e.g. NEMURO.FISH (Megrey *et al.*, 2007). For other potentially relevant models, see the Eur-Oceans MoST (Model Shopping Tool) at <http://www.eur-oceans.eu/WP3.1/Accueil/index.php>.

Layered organization in the coastal ocean

Motivation

The ultimate success of each new year class in a fishery depends on a complex mix of environmental and biological factors that affect growth and survival (Bailey *et al.*, 2005). As first recognized by Lasker (1975), the growth and survival of fish larvae often depend on their finding concentrations of plankton well above those normally detected using standard oceanographic techniques. For a fish larva, highly concentrated, vertically thin layers of plankton are probably an important feature of the ecosystem. Such layers might be discovered by just swimming up or down in the water column. Finding such a layer in a low-food environment could mean life or death for an individual larva. For a population, the widespread presence and persistence of such layers at the time of first feeding could mean the difference between a good year class and a very poor one (Bailey and Macklin, 1994). Optical and acoustic sensors are being used to detect <1 m thick layers containing high concentrations of phytoplankton and mesozooplankton and to gather detailed information on processes that result in their formation and destruction. Such information could allow predictions of when and where such concentrations of food might be available at critical life stages of fish.

In summer 2005, an interdisciplinary group undertook an intensive study of thin layers at a site 20 m deep in Monterey Bay, CA, USA (36°56.02'N 121°55.49'W). The researchers examined fine-scale layering of phytoplankton and zooplankton in relation to each other and their environment. To illustrate the use of acoustic and bio-optical profilers in this study, data from a single 24 h interval beginning at noon on 26 August 2005 have been selected. All times are in Pacific Daylight Time (PDT).

Acoustics: multifrequency volume-scattering strengths (S_v)

The TAPS ("Tracor Acoustic Profiling System") is an acoustic zooplankton sensor. In Monterey Bay, a TAPS-6 was configured as a bottom-mounted, battery-powered, upward-looking, six-frequency echosounder (Holliday *et al.*, 2003). VHF radios were used to transmit the TAPS-6 data to shore in real time, monitor the sensors, and vary the sampling rates to conserve battery power when little structure was present. On 26 and 27 August 2005, volume-scattering (S_v) spectra were collected every 10 min during the day to conserve battery power. From dusk to dawn (18:00 to 06:00), when rapid changes and complex patterns were anticipated, a 2-min sampling interval was used. For the Bering Sea work an eight-frequency model, the TAPS-8, was employed to collect data at 20-min intervals. That model was specifically designed for extended use on moorings. It archived data internally and was also linked by two-way telemetry to a surface buoy via an acoustic modem, transmitting data via Iridium satellites to shore stations where it could be accessed in near real time.

Optics: multiwavelength absorption, attenuation, and scattering

Vertical profiles of centimetre-scale physical, chemical, and bio-optical structure were measured once per hour next to the TAPS mooring using an autonomous Ocean Response Coastal Analysis System (ORCAS) vertical profiler (Babin *et al.*, 2005; Sullivan *et al.*, 2005). ORCAS is a self-contained system that profiles the water column from the bottom up, by slowly reeling out a lightweight cable connected to a small bottom weight. Once it

reaches the surface, the profiler stops, transmits data to ship or shore by VHF radio, receives any new commands, and then rapidly reels in the winch cable until the profiler returns to the bottom, where it rests until the next profiling interval. Each profiler was equipped with a Seabird SBE 49 CTD, a WET Labs ac-9 (spectral absorption, scattering, and attenuation at nine wavelengths), a BB3 (spectral backscattering at three wavelengths), a Seabird SBE 43 (dissolved oxygen), and two WETstar fluorimeters, one for Chl *a* and the other for coloured, dissolved, organic matter. Optical sensors were protected from bio-fouling by copper shutters on open-faced sensors and copper intake-tubing on flow-through instrumentation. The winch reeled out cable at 3 cm s⁻¹, whereas the sensors were sampled at 6–8 Hz, resulting in ca. two samples per centimetre.

Analysis methods: acoustics

Holliday (1977), Greenlaw (1979), and Greenlaw and Johnson (1983) describe how inverse theory is used to estimate the size and abundance of plankton, micronekton, or fish from the measurements of S_v spectra. Methods and algorithms used in transforming S_v measurements into biovolume size spectra for organisms of differing shapes can also be found in Medwin and Clay (1998, pp. 461–465) or Simmonds and MacLennan (2005, pp. 284–290 and Plate 7.1). For zooplankton, Costello *et al.* (1989) discussed the comparison of inverse results and conventional sampling.

Two scattering models were used in the inverse calculation. The truncated, fluid-sphere model (Holliday, 1992) predicts sound scattering from quasi-spherical particles, e.g. small mesozooplankton, including eggs, nauplii, and many small copepods, such as *Calanus pacificus*, *Pseudocalanus* spp., or *Acartia tonsa*. The distorted-wave, Born approximation for the geometry of a mysid was used to predict scattering from elongate organisms, such as mysids and euphausiids (Holliday *et al.*, 2003).

Analysis methods: optics

Spectral data from the ac-9 were used to calculate the biomass and size composition of particulate material, using optical-inversion models (Sullivan *et al.*, 2005). First, the fine-scale vertical structure of the phytoplankton biomass, measured as chlorophyll *a* (Chl *a*) concentration, was calculated from ac-9 measurements of absorption using the baseline-subtraction method of Davis *et al.* (1997) and a chlorophyll *in vivo* specific absorption of 0.014 m² mg⁻¹ (Bricaud *et al.*, 1995):

$$\text{Chl } a \text{ (mg m}^{-3}\text{)} = \frac{a_{\text{pg}}(676) - a_{\text{pg}}(650)}{0.014}.$$

The fine-scale structure of the size composition of particulate material was calculated from ac-9 measurements of attenuation using the hyperbolic model of Boss *et al.* (2001). This model is based on the observation that the spectral slope of the particulate attenuation coefficient (c_p) decreases with increasing dominance of large particles (Kitchen *et al.*, 1982). This slope was calculated by least-squares fit over five of the ac-9 wavelengths (440, 488, 532, 555, and 630 nm) according to the hyperbolic model of Boss *et al.* (2001):

$$c_p(\lambda) = A_c \lambda^{-\gamma}, \quad (1)$$

where λ is the wavelength, A_c an amplitude, and γ the hyperbolic slope of the attenuation spectrum (Twardowski *et al.*, 2001;

Sullivan *et al.*, 2005). The hyperbolic slope (γ) was used to estimate the slope ξ of the relative particle size distribution (PSD). The PSD is a function of $D^{-\xi}$, where D is the particle diameter, and its slope is obtained from the inversion model of Boss *et al.* (2001):

$$\xi = \gamma + 3 - 0.5 \exp(-6\gamma). \quad (2)$$

TAPS-6 observations and results

At sunset, scattering began to increase at depths of 1–2 m (Figure 1a; “*” at 19:45 PDT). Some migrators dispersed throughout the water column. During the night, scattering tended to decrease with depth and heterogeneity appeared to be greater in the lower half of the water column. Two discrete, rapid downward migrations were observed (ca. 20:56 and 21:10). Some of the migrators stopped at the 14.2°C isotherm, where they formed a thin layer that followed the isotherm closely until ca. 22:45, whereafter the layer began to broaden. Scatterers in this layer appeared to start gradually returning to the surface at ca. 23:00, with the upward migration starting in earnest just after midnight. Other migrators formed a second thin layer, eventually settling on the 13.0°C isotherm at ca. 23:30. Those scatterers closely followed this isotherm until leaving it at ca. 01:45, quickly heading for the surface, as a packet of internal waves passed over the TAPS. Scattering throughout the water column returned to daytime levels before 03:00.

A short interval just before midnight was selected as typical of the night-time vertical pattern for S_v (23:54 and 24:00; arrow, Figure 1a). These data are used to illustrate the kind of information obtained by inverse processing, namely the distribution of the water-column biomass and estimates of the shape and size of organisms participating in the night-time migration. For this 6-min interval, inverse processing revealed multiple size classes of quasi-spherical sound scatterers in the water column, three associated with the 14.2°C isotherm (0.11–1.05, 1.15–1.34, and 2.1 mm) and one with the 13.0°C isotherm (between 2.85 and 4.17 mm; Figure 1b). A biovolume peak (<1.05 mm) was also located just below the surface. The size spectrum for scatterers with elongate shapes was characterized by two peaks (Figure 1c). The smaller of these, between 17.6 and 18.0 mm, was at the depth of the shallow, thin layer of acoustic scatterers on the 14.2°C isotherm. The larger peak fell in the size bin between 20.2 and 20.6 mm, but it was distributed (Figure 1c) well above the 14.2°C isotherm.

Based on net and pump sampling, average zooplankton abundances were quite low throughout the water column, with most of the zooplankton residing in the top metre during daylight. Pump samples collected by day within a metre of the surface, and oblique day- and night-time net tows included nauplii (<0.5 mm long), the copepod *A. tonsa* (0.86 and 1.2 mm long), a few eggs (0.1 to 0.5 mm diameter), and a 1.8-mm long ostracod. The only large zooplankters collected with our net were two mysids, ca. 20 and 24 mm long, a crab megalops (18 mm across the carapace laterally), and some parts of polychaete worms.

Comparing the collected samples with the results of the inverse calculations revealed the following. The smallest of the acoustically determined, quasi-spherical size classes, 0.11–1.05 mm, contained various nauplii and eggs. The copepod *A. tonsa* appeared as two size classes in the pump samples. The first of these at 0.86 mm total length, was in the smallest size class. Biovolume peaks at those

size classes were located just below the surface and in the upper 5 m. Larger *A. tonsa* (1.2 mm) were found in the second biovolume peak (1.15–1.34 mm). These scatterers were found in both thin layers. The third peak in the size spectrum corresponded to the size of the fish eggs collected. The shallower of the thin layers contained organisms estimated at between 2.85 and 4.17 mm long, but there were no captures to explain the biovolume peak. Organisms with the shape and size of the two collected mysids would explain the two peaks in the inverse predictions for the elongate scatterers. Because there is no appropriate model to predict the scattering from the crab megalopa, its location in the computed size spectrum is uncertain, nor is it certain whether its presence was sufficient to be detected acoustically.

ORCAS observations and results

Data collected by the nearby ORCAS profiler were analysed to understand the mechanisms and effects of the formation of the thin zooplankton layers on the 13.0 and 14.2°C isotherms. Hourly ORCAS profiles on those days showed that the Chl *a* layer consistently resided at the surface during daylight, migrating into the water column each night, but with a different timing than was the case for the zooplankton migration. Water samples revealed that the migrators responsible for the Chl *a* layer were dinoflagellates, *Akashiwo sanguinea*. Chemical sensors deployed on a slow-drop platform indicated that the nightly limit of downward migration for *A. sanguinea* was the nutricline. In contrast to the two thin zooplankton layers observed at midnight, the phytoplankton formed an intense thin layer at the base of the thermocline (Figure 1d). In the midnight ORCAS profile for 26–27 August, Chl *a* levels of 1–2 $\mu\text{g l}^{-1}$ in the upper 5 m rose to a peak of 32 $\mu\text{g l}^{-1}$, then rapidly declined to <2 $\mu\text{g l}^{-1}$ in the bottom 5 m. Particle size varied in a similar fashion, increasing from small particles in surface waters (PSD slopes >3.9) to large particles at the centre of the thin chlorophyll layer (3.1 < PSD slope < 3.2), then decreasing to dominance by very small particles in deep waters (PSD slope > 4.0). In addition to this primary, thin chlorophyll layer dominated by large particles, there was a secondary layer at 6.5-m depth, evident as a secondary peak in PSD slope and as a shoulder on the Chl *a* peak, with slightly elevated biomass (3 $\mu\text{g l}^{-1}$) and intermediate particle-size characteristics. Although it might be expected that the zooplankton would migrate downwards to feed on the high-biomass layer of large phytoplankton, the zooplankton formed thin layers just above and below the peak of the phytoplankton layer. The 13.0°C isotherm was at the base of the thin Chl *a* layer, and the 14.2°C isotherm was on the upper side of the Chl *a* layer, at the depth of the secondary peak in the PSD slope. Most of the scatterers avoided the centre of the thin phytoplankton layer. For example, the 1.2-mm, quasi-spherical scatterers formed thin layers just above and below the thin Chl *a* layer, but avoided the high concentrations found at the centre of the Chl *a* layer. The 17.8-mm, elongate scatterers also formed a thin layer at the depth of the secondary peak in the PSD slope, but avoided the primary thin-chlorophyll layer and the waters below it. These results clearly indicate that factors other than phytoplankton biomass (measured as Chl *a*) control the vertical-migration behaviour of these groups of zooplankton and hence the quantity and quality of food available to them (Napp *et al.*, 1988). Although it would be interesting to know the reason for such behaviour, it is already very clear that simultaneous measurements of fine-scale, physical, optical, and acoustic structure provide modellers with information to link these trophic

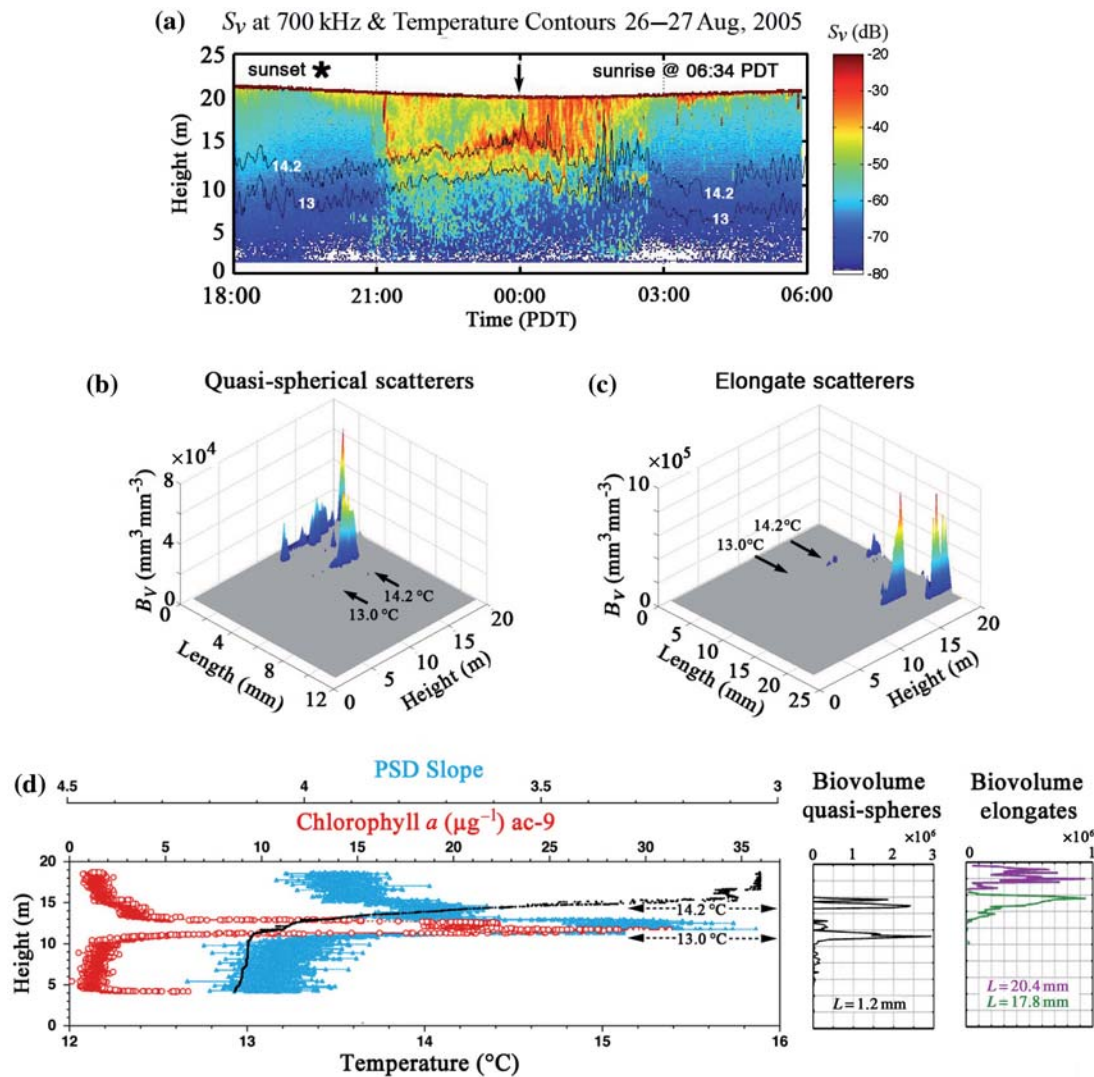


Figure 1. (a) Volume-backscattering strength (S_v , dB re 1 m^{-1}) profile pattern at 700 kHz, sampled at 2-min intervals, is overlaid by the 13.0 and 14.2°C isotherms, as measured by a 16-element t-chain <50 m from the TAPS. Sunset is marked with asterisk, and sunrise was at 06:34. Biovolume size profile for (b) quasi-spherical scatterers and (c) elongate scatterers. Both (b) and (c) were derived from S_v measured between 23:54 and 24:00, 26 August 2005, as marked by the arrow in (a). Vertical profiles of temperature (black dots), Chl a (red circles), and the slope of the spectrum of the particulate optical attenuation coefficient (blue triangles) were measured at midnight by the ORCAS profiler located next to the TAPS profiler, and are displayed in the left panel of (d). Biovolume profiles for the quasi-spherical (1.2 mm) and elongate (17.8 mm (green) and 20.4 mm (purple) scatterers are displayed on the right in panel (d).

levels and to predict the effect on the growth and survival of fish larvae that depend on the enhanced food levels found in thin layers. Equally important, the observation of such patterns during critical periods in larval or later development would be invaluable in guiding the sampling of fish-physiological condition and distribution, as well as improving knowledge of whether such avoidance is caused by the presence of toxic algae, particle size, or food quality.

Monitoring mesozooplankton and micronekton in the Bering Sea

Motivation

The Bering Sea is home to one of the world's most valuable fisheries, supplying ca. one-half of the US domestic fish harvest by weight. The Bering Sea rapidly responds to short- and long-term

climatic changes, and there is increasing evidence that these changes may reorganize the ecosystem in ways that alter stocks of living marine ecosystems and their dynamics over multiyear time-scales (Sugimoto and Tadokoro, 1997; Napp and Hunt, 2001; Orensanz *et al.*, 2004; Hunt *et al.*, 2008).

Zooplankton is critical in all marine ecosystems, providing the trophic link between primary production and apex predators, such as marine mammals, seabirds, and fish. In many high-latitude ecosystems, there is large temporal variability in zooplankton abundance and production. Superimposed on interannual and quasi-decadal variation in abundance are diel, seasonal and annual cycles. Populations in the higher trophic levels respond to these episodic highs and lows in food supply and quality. Such events affect their fecundity, as well as the survival and growth of the young. Capturing a true representation of the food available to the higher trophic levels usually requires many

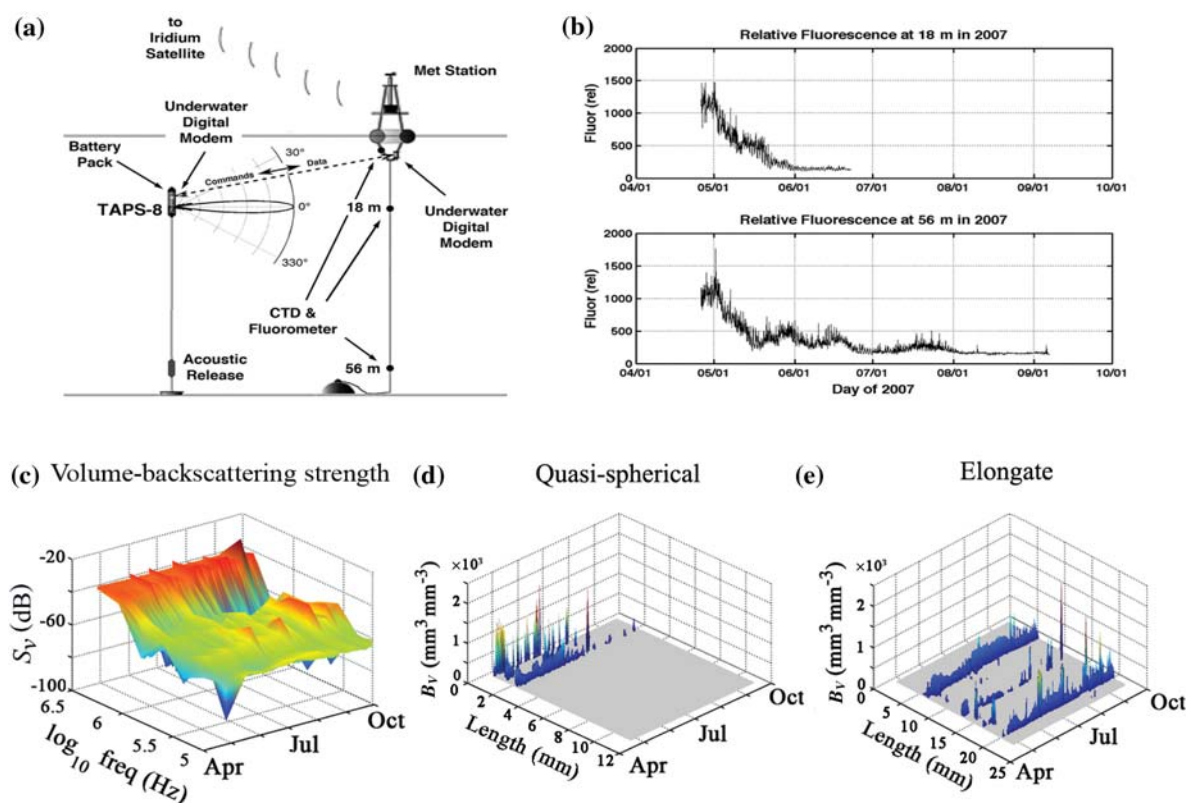


Figure 2. (a) The TAPS-8 was separately moored near a surface buoy that hosted meteorological sensors, CTDs, temperature recorders, and fluorometers. Temperature and fluorescence were measured at 18 and 56 m on the TAPS mooring. A controller on the surface buoy triggered data acquisition by the TAPS-8 at 20 min intervals via an acoustic modem. On completion of the data-acquisition cycle, the TAPS data were relayed via the acoustic modem to the surface buoy. Data from all sensors were accumulated for an hour, and a complete data packet was relayed to shore via an Iridium satellite link and distributed to the principal investigators for analysis and processing via an ftp site. (b) Fluorescence at 18 and 56 m at mooring M2. The fluorescence data from 18 m were prematurely terminated by an internal electrical problem with the sensor. Volume-backscattering strength (S_v , dB re 1 m^{-1}) vs. frequency from the Bering Sea shelf at 18 m is displayed in (c) between 25 April and 21 September 2007. The biovolume size spectra for (d) quasi-spherical and (e) elongate scatterers were both estimated from the S_v record displayed in (c).

samples collected over intervals approximating the lifetimes of the target species. In the Bering Sea and Gulf of Alaska ecosystems, it is difficult to obtain sufficient ship resources to achieve the critical levels of net sampling for zooplankton needed to detect interannual and quasi-decadal shifts in abundance and distributions. Yet, this is exactly what is required for an ecosystem approach to management and an integrated ecosystem assessment.

Here, we resolve temporal variability in zooplankton with several sensors, including an eight-frequency TAPS on a mooring (M2) at a mid-shelf location in the southeastern Bering Sea between 25 April and 21 September 2007 ($56^{\circ}51.93'\text{N}$ $164^{\circ}02.79'\text{W}$).

TAPS-8 acoustic sensor

The TAPS-8 was designed for moored operation (Figure 2a), utilizing frequencies of 104, 165, 265, 420, 700, 1100, 1850, and 3000 kHz. The “sleep-mode” power budget is exceptionally low, allowing operation for 4–6 months. Although many options are available, only measurements of S_v in a small (ca. 4 l) volume at a horizontal range of ca. 1.5 m are discussed here. As configured for the Bering Sea, the estimates of S_v were averages of backscattering from 32 pings at each frequency. Approximately

10 250 such measurements were collected between 25 April and 21 September 2007, from a depth of 18 m (Figure 2c). The interval between the ensemble averages was 20 min.

TAPS-8 observations and results

Volume-scattering spectra revealed considerable variation over time across the entire band of frequencies sampled (Figure 2c). At acoustic frequencies <700 kHz, S_v tended to be more variable than that at higher frequencies. Fluorescence at both 18 and 56 m peaked at the end of April and generally declined until late August (Figure 2b). Concentrations were quite similar at 18 and 56 m until 20 May. Thereafter, concentrations at 18 m were lower, and a series of secondary blooms was evident at 56 m in late May, mid-June, and late July. The temperatures at 18 m and near the surface were ca. 2°C at the end of April, gradually rising more or less linearly to ca. 12°C during the last half of August. Fluctuations were observed at tidal frequencies in the acoustic temperature and fluorescence records. The size-biovolume structure for the quasi-spherical particles was simple, with two size classes dominating from April to September (Figure 2d). Small quasi-spherical scatterers with lengths <0.72 mm reached peak biovolumes of $1250 \text{ mm}^3 \text{m}^{-3}$ from 27 April to 6 May. Episodic,

brief peaks in biovolume, usually small copepods, were detected at lengths <0.72 mm until mid-August, whereafter no further organisms were detected <2 mm long. Based on historical data, because direct samples were not collected, *Pseudocalanus*, *Acartia*, and *Oithona* are likely candidates for this scatterer. Biovolumes for organisms 1–2 mm long also peaked at ca. $400 \text{ mm}^3 \text{ m}^{-3}$ during a brief period of high chlorophyll fluorescence from 27 April to 6 May. Following a brief decline between 6 and 15 May, biovolumes for 2 mm organisms increased from ca. 200 to nearly $700 \text{ mm}^3 \text{ m}^{-3}$ until mid-July, whereafter only low and intermittent biovolume peaks were present with durations of a day or two, until late September.

The distribution of elongate particles was more complex, with multiple size classes present throughout the deployment period (Figure 2e). One size class (ca. 6 mm length) was continuously present, reaching a moderate peak of $470 \text{ mm}^3 \text{ m}^{-3}$ in May, during the fluorescence maximum. The average biovolume for the 6 mm size class declined to a minimum of ca. $200 \text{ mm}^3 \text{ m}^{-3}$ on 29 May, then it increased to a constant level of ca. $600 \text{ mm}^3 \text{ m}^{-3}$ until 1 August. This was followed by a rapid decline to ca. $230 \text{ mm}^3 \text{ m}^{-3}$, where it remained until the mooring was retrieved at the end of September. For 13 mm particles, the biovolume also peaked during the April–May Chl *a* maximum, but it only reached $500 \text{ mm}^3 \text{ m}^{-3}$. Periods with similar biovolume magnitudes appeared from 17 May to 20 June and 25 June to 29 July. Six, short-lived maxima (20 min or less) were detected in mid-August. The biovolume of the 20.4 mm organisms, probably euphausiids, also peaked during the late April to mid-May chlorophyll maximum. The biovolumes were low and increased gradually to a maximum level ($530 \text{ mm}^3 \text{ m}^{-3}$) that persisted from 12 June to 15 July. Those values increased sporadically to ca. $1200 \text{ mm}^3 \text{ m}^{-3}$ during that period, suggesting that there could have been patches in the area with abundances twice the average. Average biovolumes declined to ca. $100 \text{ mm}^3 \text{ m}^{-3}$, then increased to ca. $250 \text{ mm}^3 \text{ m}^{-3}$ in late September. Net samples collected near this mooring site in late September 2007 contained euphausiid furcilia of ca. 6 mm length. Historical abundance data suggest that two stages of *Thysanoessa* spp. could have been responsible for the peaks at 13 and 20.4 mm, respectively.

Summary and conclusions

Acoustic and optical systems were deployed simultaneously on the continental shelf in Monterey Bay, CA, USA, where a downward migration of mesozooplankton at dusk formed two distinct thin layers, each <0.3 m thick. These layers, which followed the 13.0 and 14.2°C isotherms for part of the evening, eventually left the isotherms and moved towards the surface. All the migrators were once again within a metre of the surface by 03:00. Profiles of six *S_v* spectra measured just before midnight were subjected to inverse processing. Each layer was found to contain mesozooplankton with essentially the same size structure as observed within a meter of the sea surface during daylight. Sensors on the ORCAS profiler revealed that a thin layer of phytoplankton, the dinoflagellate, *A. sanguinea*, had migrated to the base of the thermocline by midnight, presumably to find the nutricline. It is notable that the two thin layers of mesozooplankton were above and below the phytoplankton layer, rather than within the layer. Many reasons might explain this avoidance, with possible toxicity and cell size (70 μm) being only two; there is no technology

currently capable for remotely collecting *in situ* samples from these layers.

The deployment of the TAPS-8 on the Bering Sea shelf revealed both short- and long-term variations in mesozooplankton and micronekton abundance. The size structure of the mesozooplankton assemblage was fairly simple, whereas the micronekton appeared to have more complexity, but lower biomass. Abundance in some size classes was correlated with Chl *a*, as estimated by fluorescence, but others varied for unknown reasons. Some biovolume structure was intermittently present, but at times some size classes exhibited elevated abundances lasting for weeks. Knowledge of the periods and timing of the variations in biomass and the size structure of the plankton assemblage on the shelf, and when they happen, should facilitate attempts to determine causes and effects.

Three important conclusions result from this study. First, high-resolution sensors can be used to define critical time and space scales, by describing diel, seasonal, and intra-annual variability in phytoplankton, zooplankton, and micronekton biomass. This knowledge should result in a better understanding of processes in marine ecosystems. Second, real-time temporal and spatial information on the size and abundance of both phytoplankton and zooplankton should provide the necessary guidance for sampling to identify the critical species and measure biomass-flow rates. Last and most important, these measurements provide a basis for building models that describe the availability and specific characteristics (e.g. size and shape) of food for multiple trophic levels that include fish. Such data are important for data-driven predictive models that integrate ecosystems and their responses to natural and anthropogenic forcing that result from resource management.

Acknowledgements

The thin-layers project was sponsored by the Office of Naval Research [Awards N00014-DO-0122 (DVH) and N000140410276 (PLD)]. We gratefully acknowledge the exceptional spirit of cooperation among our colleagues in the thin layers research group. Our research in the Bering Sea was funded under NOAA AB133F07SE4862 via URI (DVH) by the North Pacific Research Board, NOAA's Climate Goal Team (North Pacific Climate Regimes and Ecosystem Productivity Project), and NOAA's Ecosystem Observation Program (IOOS Pilot Projects). We especially thank the head of the EcoFOCI mooring programme at NOAA's Pacific Marine Environmental Laboratory, P. Stabeno, and her programme scientists and engineers: Carol DeWitt, William Floering, Antonio Jenkins, and William Parker, for engineering and logistical support and deployment of the mooring and instruments. This is contribution EcoFOCI-N702 to NOAA's Ecosystems and Fishery-Oceanography Coordinated Investigations.

References

- Babin, M., Cullen, J. J., Roesler, C. S., Donaghay, P. L., Doucette, G. J., Kahru, M., Lewis, M. R., *et al.* 2005. New approaches and technologies for observing harmful algal blooms. *Oceanography*, 18: 210–227.
- Bailey, K. M., Ciannelli, L., Bond, N. A., Belgrano, A., and Stenseth, N. C. 2005. Recruitment of walleye pollock in a physically and biologically complex ecosystem. A new perspective. *Progress in Oceanography*, 67: 24–42.
- Bailey, K. M., and Macklin, S. A. 1994. Analysis of patterns in larval walleye pollock *Theragra chalcogramma* survival and wind mixing

- events in Shelikof Strait, Gulf of Alaska. *Marine Ecology Progress Series*, 113: 1–12.
- Boss, E., Twardowski, M. S., and Herring, S. 2001. Shape of the particulate beam spectrum and its inversion to obtain the shape of the particle size distribution. *Applied Optics*, 40: 4885–4893.
- Bricaud, A., Babin, M., Morel, A., and Claustre, H. 1995. Variability in the chlorophyll-specific absorption coefficients of natural phytoplankton: analysis and parameterization. *Journal of Geophysical Research*, 100: 13321–13332.
- Costello, J. H., Pieper, R. E., and Holliday, D. V. 1989. Comparison of acoustic and pump sampling techniques for the analysis of zooplankton distributions. *Journal of Plankton Research*, 11: 703–709.
- Davis, R. F., Moore, C. C., Zaneveld, J. R. V., and Napp, J. M. 1997. Reducing the effects of fouling on chlorophyll estimates derived from long-term deployments of optical instruments. *Journal of Geophysical Research*, 102: 5851–5855.
- Greenlaw, C. F. 1979. Acoustical estimation of zooplankton populations. *Limnology and Oceanography*, 24: 226–242.
- Greenlaw, C. F., and Johnson, R. K. 1983. Multiple-frequency acoustical estimation. *Biological Oceanography*, 2: 227–252.
- Holliday, D. V. 1977. Extracting bio-physical information from the acoustic signatures of marine organisms. In *Marine Science Series*, 5, *Ocean Sound Scattering Prediction*, pp. 619–624. Ed. by N. R. Anderson, and B. J. Zahuranec. Plenum Press, New York, NY. 859 pp.
- Holliday, D. V. 1992. Zooplankton acoustics. In *Oceanography of the Indian Ocean*, pp. 733–740. Ed. by B. Desai. Oxford and IBH Publishing Co. Pvt. Ltd, New Delhi.
- Holliday, D. V., Donaghay, P. L., Greenlaw, C. F., McGehee, D. E., McManus, M. M., Sullivan, J. M., and Miksis, J. L. 2003. Advances in defining fine- and micro-scale pattern in marine plankton. *Aquatic Living Resources*, 16: 131–136.
- Hunt, G. L., Stabeno, P. J., Strom, S., and Napp, J. M. 2008. Patterns of spatial and temporal variation in the marine ecosystem of the southeastern Bering Sea, with special reference to the Pribilof Domain. *Deep Sea Research II*, 55: 1919–1944.
- ICES. 2004. Report of the Thirteenth ICES Dialogue Meeting: Advancing Scientific Advice for an Ecosystem Approach to Management: Collaboration amongst Managers, Scientists, and Other Stakeholders. ICES Cooperative Research Report, 267. 59 pp.
- Kitchen, J. C., Zaneveld, J. R. V., and Pak, H. 1982. Effect of particle size distribution and chlorophyll content on beam attenuation spectra. *Applied Optics*, 21: 3913–3918.
- Lasker, R. 1975. Field criteria for survival of anchovy larvae: the relation between inshore chlorophyll maximum layers and successful first feeding. *Fishery Bulletin US*, 73: 453–462.
- Medwin, H., and Clay, C. S. 1998. *Fundamentals of Acoustical Oceanography*. Academic Press, San Diego. 712 pp.
- Megrey, B. A., Rose, K. A., Ito, S., Hay, D. E., Werner, F. E., Yamanaka, Y., and Aita, M. N. 2007. North Pacific basin-scale differences in lower and higher trophic level marine ecosystem responses to climate impacts using a nutrient–phytoplankton–zooplankton model coupled to a fish bioenergetics model. *Ecological Modelling*, 202: 196–210.
- Napp, J. M., Brooks, E. R., Matrai, P., and Mullin, M. M. 1988. The vertical distribution of marine particles and grazers. II. Relation of grazer distribution to food quality and quantity. *Marine Ecology Progress Series*, 50: 59–72.
- Napp, J. M., and Hunt, G. L. 2001. Anomalous conditions in the southeastern Bering Sea. *Fisheries Oceanography*, 10: 61–68.
- Orensanz, J., Ernst, B., Armstrong, D. A., Stabeno, P., and Livingston, P. 2004. Contraction of the geographic range of distribution of snow crab (*Chionoecetes opilio*) in the eastern Bering Sea: an environmental ratchet? *CalCOFI Report*, 45: 65–79.
- Simmonds, J., and MacLennan, D. 2005. *Fisheries Acoustics: Theory and Practice*, 2nd edn. Blackwell Science, Oxford. 437 pp.
- Sugimoto, T., and Tadokoro, K. 1997. Interannual–interdecadal variations in zooplankton biomass, chlorophyll concentration and physical environment in the subarctic Pacific and Bering Sea. *Fisheries Oceanography*, 6: 74–93.
- Sullivan, J. M., Twardowski, M. S., Donaghay, P. L., and Freeman, S. 2005. Using optical scattering to discriminate particle types in coastal waters. *Applied Optics*, 44: 1667–1680.
- Twardowski, M. S., Boss, E., Macdonald, J. B., Pegau, W. S., Barnard, A. H., and Zaneveld, J. R. V. 2001. A model for estimating bulk refractive index from the optical backscattering ratio and the implications for understanding particle composition in case I and case II waters. *Journal of Geophysical Research*, 106: 14129–14142.

doi:10.1093/icesjms/fsp127